

# Phosholenes from Phosphabenzenes by Selective Ring Contraction

Jinxiong Lin,<sup>[a]</sup> Nathan T. Coles,<sup>[a, b]</sup> Lea Dettling,<sup>[a]</sup> Luca Steiner,<sup>[c]</sup> J. Felix Witte,<sup>[c]</sup> Beate Paulus,<sup>[c]</sup> and Christian Müller\*<sup>[a]</sup>

**Abstract:** A 3-amino-functionalized phosphabenzene (phosphinine) has been synthesized and structurally characterized. The pyramidalized nitrogen atom of the dimethylamino substituent indicates only a weak interaction between the lone pair of the nitrogen atom and the aromatic phosphorus heterocycle, resulting in somewhat basic character. It turned out that the amino group can indeed be protonated by HCl.

In contrast to pyridines, however, the phosphabenzene-ammonium salt undergoes a selective ring contraction to form a hydroxylphospholene oxide in the presence of additional water. Based on deuterium labeling experiments and quantum chemical calculations, a rational mechanism for this hitherto unknown conversion is proposed.

## Introduction

$\lambda^3, \sigma^2$ -Phosphinines, also known as phosphabenzenes or phosphorines, are intriguing aromatic phosphorus heterocycles that are currently undergoing a renaissance within coordination chemistry, small-molecule activation, catalysis and molecular materials science.<sup>[1–3]</sup> However, for their use in more applied research fields, their specific functionalization is particularly important in order to modify their stereo-electronic properties and coordination abilities. Phosphinines with additional donor-substituents at the 2-position of the heterocycle (**A**, Figure 1) are relatively rare. Small bite-angle phosphinines ( $\text{Do}=\text{PR}_2$ ), for example, have been used successfully as chelating ligands in several catalytic reactions.<sup>[4]</sup> Grützmacher and co-workers have accessed sodium salts of phosphinine-2-ols ( $\text{Do}=\text{OH}$ ).<sup>[5]</sup> The anionic phosphinine-2-olate ( $\text{Do}=\text{ONa}$ ) acts as a 4e-donor and bridges a cationic  $[\text{Au}(\text{PPh}_3)]^+$  and a neutral  $[\text{AuCl}]$  fragment.<sup>[6]</sup> We have recently reported the first 2-*N,N*-dimethylaminophosphinine **B**. Natural resonance theory calculations

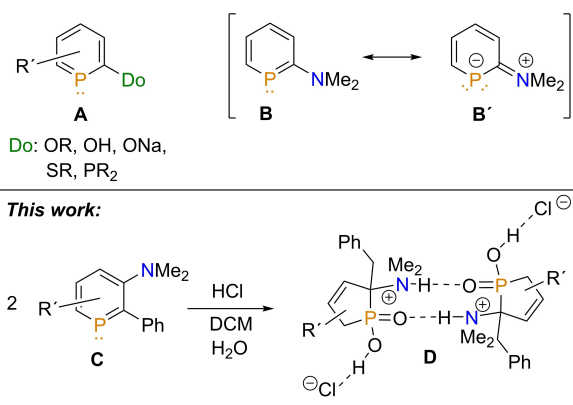


**Figure 1.** 2-Donor-substituted phosphinines and a pictorial summary of this work.

revealed resonance structures with two lone-pairs at the phosphorus atom (**B'**), contributing substantially to the electronic ground state of this compound. Accordingly, **B/B'** forms coordination polymers with  $\text{CuBr}\cdot\text{S}(\text{CH}_3)_2$ , in which the phosphorus atom of the phosphinine heterocycle bridges two  $\text{Cu}^I$  centers in a rare  $\mu_2$ -P-4e coordination mode in the solid state, exhibiting the first example for this bonding motif for a neutral substituted phosphinine.<sup>[7]</sup>

Stimulated by these results, we anticipated to synthesize a 3-amino-functionalized phosphinine (**C**) with the aim to investigate the influence of an amino group in 3-position on the electronic properties and the reactivity of the corresponding phosphorus heterocycle. We report here an unusual ring contraction of **C** in the presence of hydrochloric acid and water and the selective formation of a hydroxylphospholene oxide (**D**, Figure 1).

[a] J. Lin, Dr. N. T. Coles, L. Dettling, Prof. Dr. C. Müller  
Freie Universität Berlin  
Institut für Chemie und Biochemie  
Fabeckstrasse 34/36, 14195 Berlin (Germany)  
E-mail: c.mueller@fu-berlin.de

[b] Dr. N. T. Coles  
School of Chemistry, University of Nottingham  
University Park, Nottingham NG7 2RD (UK)

[c] L. Steiner, Dr. J. Felix Witte, Prof. Dr. B. Paulus  
Freie Universität Berlin  
Institut für Chemie und Biochemie  
Arnimallee 22, 14195 Berlin (Germany)

Supporting information for this article is available on the WWW under <https://doi.org/10.1002/chem.202203406>

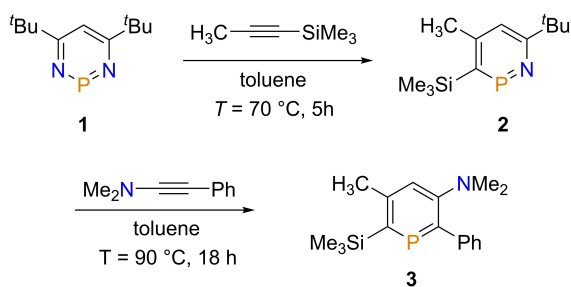
© 2022 The Authors. Chemistry - A European Journal published by Wiley-VCH GmbH. This is an open access article under the terms of the Creative Commons Attribution Non-Commercial License, which permits use, distribution and reproduction in any medium, provided the original work is properly cited and is not used for commercial purposes.

## Results and Discussion

While **B** was prepared by the 2-pyrone route, we found that the 3-*N,N*-dimethylaminophosphinine derivative **3** can easily be synthesized by using a method developed by Mathey and co-workers.<sup>[8]</sup> The precursor 1,3,2-diazaphosphinine (**1**) was sequentially reacted with 1-(trimethylsilyl)propyne to afford azaphosphinine **2** and subsequently with *N,N*-dimethyl-phenylacetylene at elevated temperatures in toluene (Scheme 1).

A single resonance at  $\delta(\text{ppm}) = 244.0$  was found for product **3** in the  $^{31}\text{P}\{^1\text{H}\}$  NMR spectrum. The chemical shift is remarkably different compared to the one observed for the previously synthesized phosphinine **B** ( $\delta(\text{ppm}) = 127.0$ ). This already indicates, that the electronic properties of **3** vary significantly from its regioisomer. Crystals of **3** suitable for single-crystal X-ray diffraction were obtained by slow evaporation of the solvent from a solution of **3** in *n*-hexanes and the molecular structure of this compound in the solid state is depicted in Figure 2, along with selected bond lengths and angles.

The crystallographic characterization of **3** shows, that the N(1)–C(4) bond length of 1.406(1) Å is closer to a C–N single bond (1.47 Å) than to a double bond (1.28 Å).<sup>[9]</sup> Moreover, the nitrogen atom of the dimethylamino substituent in **3** is pyramidalized ( $\Sigma \chi(\text{CNC}) = 345.9^\circ$ ), in contrast to the bonding observed for **B/B'** in a  $\text{Cu}^{\text{I}}$  complex, in which the phosphinine serves as a ligand. The twist angle of best plane through the



**Scheme 1.** Synthesis of the 3-*N,N*-dimethylamino-functionalized phosphinine **3**.

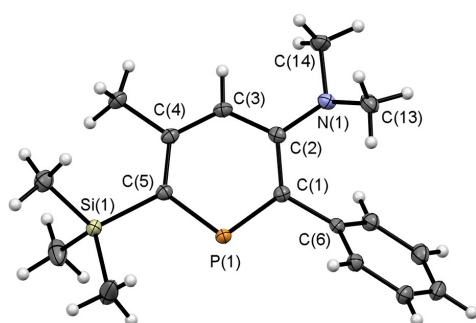


**Figure 2.** Molecular structure of **3** in the crystal. Displacement ellipsoids are shown at the 50% probability level. Selected bond lengths [Å] and angles [°]: P(1)–C(1): 1.7369(8), P(1)–C(5): 1.7333(8), N(1)–C(2): 1.4059(10), C(1)–C(2): 1.4151(11), C(2)–C(3): 1.4104(11), C(3)–C(4): 1.3960(12), C(4)–C(5): 1.4115(11), C(1)–P(1)–C(5): 105.33(4), C(2)–N(1)–C(14): 118.06(7), C(2)–N(1)–C(13): 117.58(7), C(13)–N(1)–C(14): 110.26(7).

NMe<sub>2</sub> group versus the phosphinine ring has been calculated as 28.30(5)°. For **3**, this might hint to only a weak electronic interaction between the nitrogen lone pair and the  $\pi$ -accepting phosphorus heterocycle.

As shown by us recently, an *N,N*-dimethylamino group in the 2-position of the parent phosphinine induces accumulation of negative charge (red) in the ring of the  $\pi$ -system, as visualized by the electrostatic potential (ESA) map of **B/B'** (Figure 3, left).<sup>[7]</sup> In this case, the ring is even more negative than the nitrogen substituent, in full accordance with the  $\pi$ -accepting character of the aromatic phosphorus heterocycle. Accordingly, the basicity of **B/B'** is also reduced with respect to *N,N*-dimethylaniline, as shown by a decrease of the computed gas phase basicities (220 kcal mol<sup>−1</sup> for **B/B'** versus 225 kcal mol<sup>−1</sup> for C<sub>6</sub>H<sub>5</sub>N(CH<sub>3</sub>)<sub>2</sub>).

In contrast, according to the electrostatic potential map of **3**, we found a large concentration of electrons close to the nitrogen atom, suggesting the presence of a lone pair that is not part of the aromatic phosphorus heterocycle (Figure 3, right). Interestingly, this effect is clearly caused by the steric demand of the phenyl- group in the 2-position of **3**. In fact, the parent phosphinine, substituted in 3-position by an *N,N*-dimethylamino group (**3'**), shows again a fully planar nitrogen atom (Figure S29 in the Supporting Information). Consequently, because the lone pair of the nitrogen atom in **3** shows only weak interaction with the aromatic system, the amino substituent should provide a stronger basic character than the one in **B/B'**. This is also confirmed by the calculated gas phase basicity of this compound (225 kcal mol<sup>−1</sup> for **3** vs. 220 kcal mol<sup>−1</sup> for **B/B'**).<sup>[10]</sup>

We thus anticipated, that the amine functionality in **3** can easily be protonated, in contrast to **B/B'**. Upon addition of a slight excess of HCl/Et<sub>2</sub>O to **3**, a precipitate is formed instantaneously. Based on the  $^1\text{H}$  and  $^{31}\text{P}$  NMR data, the protonated species **4** is formed initially, with the SiMe<sub>3</sub>-substituent still located in the *ortho* position of the heterocycle. The signal of this protonated species **4** can be found at  $\delta(\text{ppm}) = 252.3$  in the  $^{31}\text{P}\{^1\text{H}\}$  NMR spectrum. However, during the process

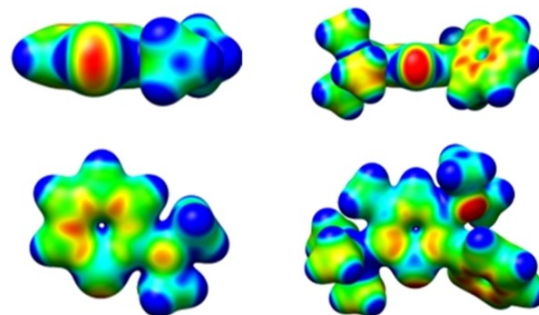
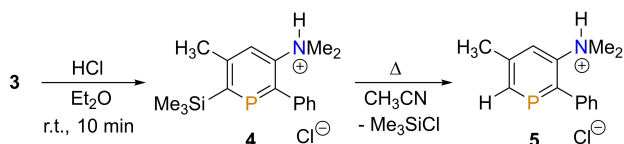


**Figure 3.** Electrostatic potential maps for **B/B'** (left) and **3** (right). Parameters:  $r(\text{red})$ : 0.000, yellow: 0.025, green: 0.050, light blue: 0.075, blue 0.100. The electrostatic potential [a.u.] is mapped on electron density isosurfaces of 0.02 e au<sup>−3</sup>. The calculations were performed at a B3LYP-D3/def2-TZVP level.<sup>[7]</sup>

of recrystallizing **4** from hot acetonitrile, protodesilylation occurs, resulting in phosphinine **5** (Scheme 2).

Compound **5** shows a single resonance at  $\delta(\text{ppm}) = 212.7$  in the  $^{31}\text{P}\{\text{H}\}$  NMR spectrum. The crystallographic characterization of **5** (Figure 4) displays indeed the presence of an ammonium group in the 3-position of the phosphinine as well as a  $\text{Cl}^-$  counter anion, and clearly shows that protodesilylation had occurred.

Surprisingly, when the suspension containing the white precipitate is stirred for a prolonged time at room temperature in an open reaction vessel, a clear solution is formed overnight at room temperature. The  $^{31}\text{P}\{\text{H}\}$  NMR spectrum shows that a new compound had formed selectively, which exhibits a single signal at  $\delta(\text{ppm}) = 53.0$ . Remarkably, this chemical shift is not in the usual range found for a phosphinine, which indicates that there is no  $\lambda^3, \sigma^2$ -phosphinine present anymore.<sup>[11]</sup> Crystals of the product (**6**; Scheme 3) suitable for X-ray diffraction were



Scheme 2. Synthesis of protonated phosphinines **4** and **5**.

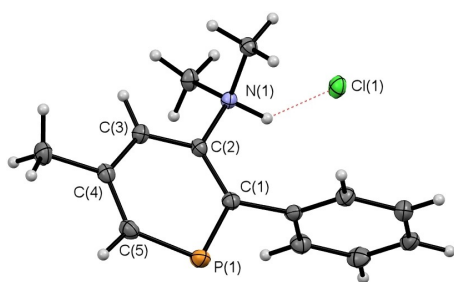
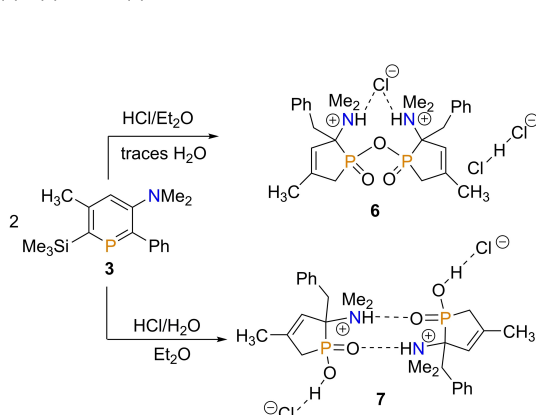


Figure 4. Molecular structure of **5** in the crystal. Displacement ellipsoids are shown at the 50% probability level. Selected bond lengths [Å] and angles [°]: P(1)–C(1): 1.7445(13), P(1)–C(5): 1.7230(14), C(1)–C(2): 1.3886(17), C(2)–C(3): 1.3942(16), C(3)–C(4): 1.3940(17), C(4)–C(5): 1.3902(18), N(1)–C(2): 1.4824(15), C(1)–P(1)–C(5): 102.13(6).



Scheme 3. Formation of oxygen-bridged phospholene oxide **6** and hydroxylphospholene oxide **7**.

obtained from a concentrated solution of **6** in a mixture of dichloromethane and *n*-hexane. The molecular structure of **6** in the solid state is depicted in Figure 5, along with selected bond lengths and angles.

Much to our surprise, the crystallographic characterization of **6** reveals that the product consists of two phospholene oxide moieties bridged by an additional oxygen atom. The amine functionalities of both five-membered phosphorus heterocycles are protonated, with the chloride counter anion bridging the two ammonium groups by hydrogen bonding. The second counter anion is a rare hydrogen dichloride anion  $[\text{Cl}(\text{HCl})^-]$ , which is located on the unit cell with the bond lengths matching those previously reported in literature.<sup>[12]</sup>

The P(1)–C(1) (1.80 Å) and P(1)–C(4) (1.86 Å) bond lengths are consistent with those of reported phospholenes.<sup>[13]</sup> In general, hydrogen dichloride salts tend to liberate HCl readily with some of them being rather unstable toward moisture and oxygen.<sup>[14]</sup> **6**, however, is air and moisture stable in solution and in the solid state. While ring expansion reactions from phospholes to phosphinines and a ring contraction from 1,3,5-triphosphinines to a triphosphole have been reported in literature before, the here presented results are the first case of a ring contraction reaction from a 1-phosphinine to a hydroxylphospholene oxide.<sup>[15,16]</sup>

To clarify the role of water in this reaction (see also Figures S25 and S26), a dry solution of HCl/Et<sub>2</sub>O was reacted with a solution of **3** in diethyl ether and monitored by means of NMR spectroscopy. Again, a precipitate was formed immediately and no resonance could be observed in the  $^{31}\text{P}\{\text{H}\}$  spectrum anymore. The white precipitate is, however, soluble in CD<sub>3</sub>CN and the NMR spectra verified the formation of the protonated species **4**. When dichloromethane was used as a solvent, the first step in the protonation of **3** with HCl/Et<sub>2</sub>O is again the formation of **4**. A prolonged reaction time leads to a new, yet unknown transient intermediate with a resonance at  $\delta(\text{ppm}) = 75.0$  in the  $^{31}\text{P}\{\text{H}\}$  NMR spectrum. Finally, protodesilylation occurs and **5** is formed quantitatively. Apparently, the presence of water is indeed essential for the ring contraction to

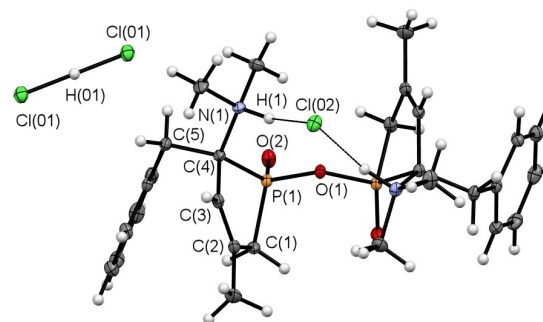
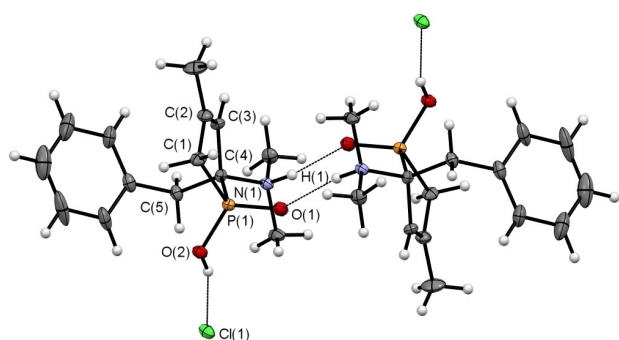


Figure 5. Molecular structure of **6** in the crystal. Displacement ellipsoids are shown at the 50% probability level. Selected bond lengths [Å] and angles [°]: P(1)–C(1): 1.7956(13), P(1)–C(4): 1.8629(12), P(1)–O(1): 1.6307(6), P(1)–O(2): 1.4687(9), N(1)–C(4): 1.5225(15), N(1)–H(1): 0.980, C(1)–C(2): 1.5137(18), C(2)–C(3): 1.3381(18), C(3)–C(4): 1.5110(17), C(4)–C(5): 1.5542(16), C(1)–P(1)–C(4): 95.89(6), P(1)–O(2)–P(1): 121.92(8).

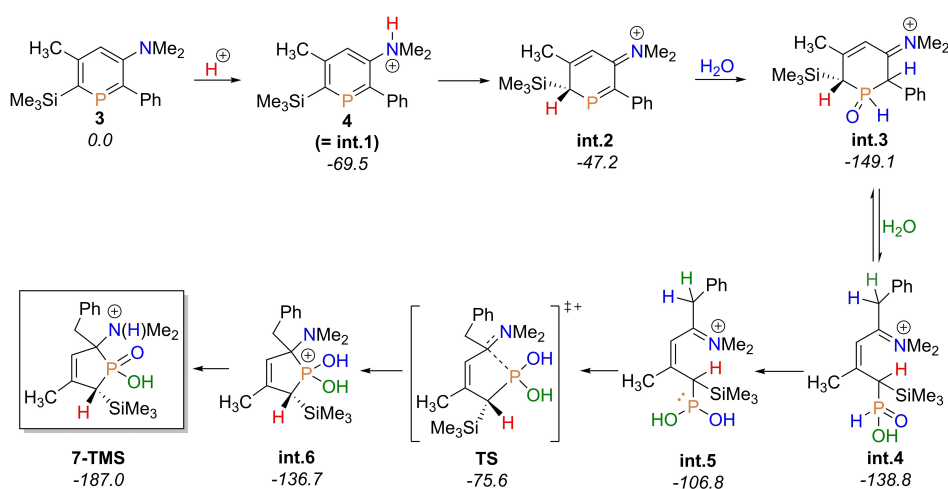
occur, while in the absence of water only protonation, followed by protodesilylation, occurs.<sup>[17]</sup>

Consequently, we attempted the reaction of **4** with an aqueous HCl solution in dichloromethane. The main product showed a resonance at  $\delta(\text{ppm})=56.0$  in the  $^{31}\text{P}\{\text{H}\}$  NMR spectrum after stirring the reaction mixture for overnight. The chemical shift of this species is similar to the one recorded for the oxygen bridged dimer **6**, however, not identical. According to NMR spectroscopic analysis, it was identified as compound **7-TMS**. Recrystallization of this species from a hot isopropanol solution afforded crystals suitable for X-ray diffraction and the molecular structure of **7** (Scheme 3) is depicted in Figure 6, along with selected bond lengths and angles.

The crystallographic characterization of **7** shows that the product consists again of a five-membered phosphorus heterocycle. In contrast to **6**, however, a hydroxyphospholene oxide is present, that forms hydrogen bonding to a second molecule, via the  $-\text{P}=\text{O}$  and  $-\text{N}(\text{H})\text{Me}_2$  moieties.



**Figure 6.** Molecular structure of **7** in the crystal. Displacement ellipsoids are shown at the 50% probability level. Selected bond lengths [Å] and angles [°]: P(1)-C(1): 1.786(3), P(1)-C(4): 1.863(3), P(1)-O(1): 1.483(3), P(1)-O(2): 1.550(3), N(1)-C(4): 1.533(4), N(1)-H(1): 0.93(5), C(1)-C(2): 1.515(5), C(2)-C(3): 1.333(5), C(3)-C(4): 1.507(5), C(4)-C(5): 1.548(5); C(1)-P(1)-C(4): 95.78(16).



**Scheme 4.** Proposed mechanism for the reaction of **3** with HCl in the presence of water. **7-TMS** is the main product; relative Gibbs free energies [ $\text{kJ mol}^{-1}$ ] are given below the compound name. Calculated at the PBE0-D3(BJ) level of theory. Int.: intermediate. Note: only the diastereomer **int.3** is shown as **int.3'** is located at higher energy ( $-146.4 \text{ kJ mol}^{-1}$ ) and therefore not considered for the mechanism.

Moreover, protodesilylation occurred during the reaction or the crystallization process, respectively. The dissolved crystals show a signal in the  $^{31}\text{P}\{\text{H}\}$  NMR spectrum at  $\delta(\text{ppm})=47.0$ . Formally, **7** is the hydrolyzed product of the oxygen-bridged dimer **6** (Scheme 3).

In order to get insight into the mechanism of the formation of **7-TMS** (or **7**), calculations based on Grimme's PBEH-3c composite method<sup>[18]</sup> and the PBE0-D3(BJ)<sup>[19]</sup> level of DFT were carried out (see the Supporting Information). Based on the computational results, the NMR monitoring experiments as well as the crystallographic data, we propose the following mechanism for the ring contraction in the presence of water (Scheme 4). The first step is the protonation of the amino substituent by HCl, forming **4** as the first intermediate (**int.1**).

This step is exergonic by  $-69.5 \text{ kJ mol}^{-1}$  and fully consistent with the NMR experiments. A proton migration forming a racemic mixture of **int.2** occurs, which is energetically feasible under the applied reaction conditions ( $+22.3 \text{ kJ mol}^{-1}$ ). Subsequently, we propose the addition of water to the reactive  $\text{P}=\text{C}$  bond in **int.2** to give a trivalent hydroxyphosphine species (HOPCH(Ph)R), that tautomerizes to **int.3**. Overall, this process is also exergonic by  $-101.9 \text{ kJ mol}^{-1}$ . A related tautomerism reaction at a phosphinine has been reported in the literature before.<sup>[20]</sup> Moreover, metal complexes of phosphinines also readily add  $\text{H}_2\text{O}$  across the  $\text{P}=\text{C}$  double bond.<sup>[21]</sup>

In the presence of a second water molecule, **int.3** is in equilibrium with the phosphinic acid derivate **int.4** ( $+8.7 \text{ kJ mol}^{-1}$ ). **Int.4** can transform into tautomer **int.5** ( $+32.0 \text{ kJ mol}^{-1}$ ). Such a process is known in literature.<sup>[22]</sup> The formation of **int.5** is crucial in order to reach the transition state of the rate-determining step (RDS). The phosphorus atom in **int.5**, having a rather strong nucleophilicity, can react with electrophilic  $\text{C}=\text{N}^+$  moieties intermolecularly to form a new  $\text{P}-\text{C}$  bond. The formation of the  $\text{P}-\text{C}$  bond ( $+33.3 \text{ kJ mol}^{-1}$ ) in the transition state (**TS**) can be specified as a 5-*exo-trig* reaction, which is allowed according to the Baldwin rules.<sup>[23]</sup> The ring

formation from **TS** to **int.6** is associated with a significant decrease in free energy by  $-63.2 \text{ kJ mol}^{-1}$ . The last step is a proton transfer, which is a significantly exergonic reaction ( $-50.3 \text{ kJ mol}^{-1}$ ), to form the final product **7-TMS**. The whole reaction sequence is exergonic by  $-187.0 \text{ kJ mol}^{-1}$  and the energy barrier of the RDS (**int.3**→**TS**) is  $76.0 \text{ kJ mol}^{-1}$ . The protodesilylation to **7** presumably proceeds in the presence of excess HCl during the recrystallization process.

In order to get additional experimental proof for our proposed mechanism, we sought to incorporate deuterium into the products by using DCl/D<sub>2</sub>O. The reaction between **3** and DCl/D<sub>2</sub>O in dichloromethane was stirred for overnight. The product (**7-d**) was recrystallized from hot isopropanol. For compound **7-d** several signals (Figure S22) can be detected as broad resonances due to <sup>2</sup>D,<sup>13</sup>C coupling in the <sup>13</sup>C{<sup>1</sup>H} NMR spectrum compared to that of compound **7**.

Moreover, compound **7 d** shows a chemical shift ( $\delta$ (ppm) = 47.5) similar to compound **7** in the <sup>31</sup>P{<sup>1</sup>H} NMR spectrum. By means of 2D and HMQC NMR experiments, the D-atoms were assigned to the positions depicted in Scheme 5, which supports the proposed mechanism. Moreover, the crystallographic characterization of **7-d** showed the same molecular structure in the solid state as determined for **7**.

It is clear, that the unusual ring-contraction reaction can only proceed due to the special electronic properties of phosphinines in combination with the reactivity of low-coordinate organophosphorus species. This indeed allows sequential reactions at the aromatic phosphorus heterocycle, in contrast to functionalized pyridines.

## Conclusion

In summary, we have synthesized and structurally characterized a new 3-amino-functionalized phosphinine by a series of [4 + 2] cycloaddition/cycloreversion reactions, starting from 1,3,2-diazaphosphinine, 1-(trimethylsilyl)propyne and *N,N*-dimethyl-phenylacetylene. The steric demand of the phenyl group in the  $\alpha$ -position of the heterocycle causes a weak electronic interaction between the nitrogen lone pair and the aromatic phosphorus heterocycle, as evidenced by a substantial pyramidalization of the nitrogen atom. This allows protonation of the dimethylamino substituent by hydrochloric acid. Remarkably, in the presence of water, the protonated phosphinine undergoes a hitherto unknown, selective ring contraction to form a hydroxyphospholene oxide that participates in hydrogen bonding and forms a dimer in the solid state. DFT-based calculations and

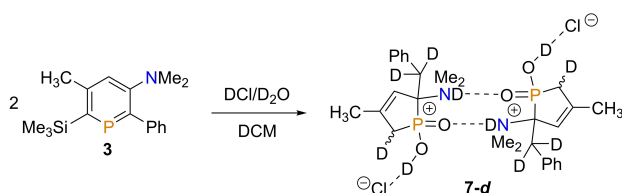
deuterium labeling experiments were performed to gain insight into the reaction mechanism. The experimental results are fully consistent with the calculations and the proposed reaction pathway. Overall, we could show for the first time that a phosphinine can undergo a selective and quantitative ring contraction reaction. The special electronic properties of phosphinines in combination with the particular reactivity of low-coordinate organophosphorus species allow sequential reactions at the aromatic phosphorus heterocycles, in contrast to functionalized pyridines.

## Experimental Section

**General:** All reactions were performed under argon in oven-dried glassware by using modified Schlenk techniques unless otherwise stated. All common solvents and chemicals were commercially available and were used without further purification. All dry or deoxygenated solvents were prepared using standard techniques or were used from a MBraun solvent purification system. *N,N*-dimethyl-2-phenylethyn-1-amine and 1,3,2-diazaphosphinines were prepared according to literature.<sup>[8,24]</sup> The <sup>1</sup>H, <sup>19</sup>F, <sup>13</sup>C{<sup>1</sup>H}, <sup>31</sup>P{<sup>1</sup>H} and <sup>31</sup>P NMR spectra were recorded on a JEOL ECX400 (400 MHz) spectrometer and a Bruker Avance 600 (600 MHz), and all chemical shifts are reported relative to the residual resonance in the deuterated solvents. The HRMS ESI mass spectra were measured on an Agilent 6210 ESI-TOF. Low-temperature X-ray diffractometry was performed on a Bruker-AXS X8 Kappa Duo diffractometer with *l* $\mu$ S micro-sources, performing  $\phi$  and  $\omega$  scans. Data were collected by using a Photon 2 CPAD detector with Mo<sub>K $\alpha$</sub>  radiation ( $\lambda = 0.71073 \text{ \AA}$ ).

**Synthesis of 3:** 1 equiv. of 1-(trimethylsilyl)prop-1-yne (0.22 g, 2.0 mmol) was added to a solution of 1,3,2-diazaphosphinine (2.0 mmol, 0.13 M) in toluene (15 mL). The mixture was heated at  $T = 70^\circ\text{C}$  for 5 h after which complete formation of the 1,2-monoazaphosphinine was observed by <sup>31</sup>P NMR spectroscopy ( $\delta = 297.9 \text{ ppm}$ ). Next, 2 equiv. of *N,N*-dimethyl-2-phenylethyn-1-amine (0.58 g, 4 mmol) were added to the mixture and heated at  $T = 90^\circ\text{C}$  for overnight. The solution was cooled to room temperature and the product purified by column chromatography (silica) using an eluent of *n*-hexane/ethyl acetate (9:1). Yield: 78% (471 mg, 1.56 mmol). <sup>1</sup>H NMR (400 MHz, C<sub>6</sub>D<sub>6</sub>):  $\delta = 7.65$  (d, <sup>1</sup>J<sub>H,H} = 7.8 Hz, 2H, 1-Ph), 7.24 (t, <sup>1</sup>J<sub>H,H} = 7.5 Hz, 2H, -Ph), 7.11 (td, <sup>1</sup>J<sub>H,H} = 7.4, 1.3 Hz, 1H, -Ph), 6.78 (brs, 1H, C<sub>5</sub>HP), 2.45 (s, 3H, -Me), 2.33 (s, 6H, -NMe<sub>2</sub>), 0.48 ppm (d, <sup>4</sup>J<sub>H,P} = 1.8 Hz, 9H, -TMS); <sup>13</sup>C{<sup>1</sup>H} NMR (151 MHz, C<sub>6</sub>D<sub>6</sub>):  $\delta = 156.8$  (d, <sup>1</sup>J<sub>C,P} = 88 Hz), 156.3 (d, <sup>1</sup>J<sub>C,P} = 106 Hz), 155.9 (d, <sup>2</sup>J<sub>C,P} = 10 Hz), 149.7 (d, <sup>2</sup>J<sub>C,P} = 13 Hz), 143.7 (d, <sup>2</sup>J<sub>C,P} = 24 Hz), 129.3 (d, <sup>3</sup>J<sub>C,P} = 11 Hz), 128.7 (s), 126.6 (s), 122.9 (d, <sup>3</sup>J<sub>C,P} = 16 Hz), 42.6 (s), 26.3 (d, <sup>4</sup>J<sub>C,P} = 3 Hz), 1.5 ppm (d, <sup>3</sup>J<sub>C,P} = 11 Hz); <sup>31</sup>P{<sup>1</sup>H} NMR (162 MHz, C<sub>6</sub>D<sub>6</sub>):  $\delta = 244 \text{ ppm}$ ; HR-ESI MS (*m/z*): 302.1506 (calcd: 302.1489) [*M* + H]<sup>+</sup>; Element analysis calculated (%) for C<sub>17</sub>H<sub>24</sub>NPSi: C 67.74, H 8.03, N 4.65; found: C 67.79, H 9.519, N 4.672.</sub></sub></sub></sub></sub></sub></sub></sub></sub></sub></sub></sub></sub>

**Synthesis of 4:** Compound **3** (36 mg, 0.12 mmol) was dissolved in 2 mL Et<sub>2</sub>O at room temperature, and 0.1 mL HCl in water (0.24 mmol, 2.4 M) was added to the Schlenk flask. A white precipitate was formed immediately, after which the reaction was stirred for an additional 10 min. All solvents were removed by syringe and the residual solid was washed with Et<sub>2</sub>O. Yield: 75% (30 mg, 0.09 mmol). <sup>1</sup>H NMR (400 MHz, CD<sub>3</sub>CN):  $\delta = 7.68\text{--}7.00$  (m, 6H, C<sub>5</sub>HP, 1-Ph), 3.26–2.82 (m, 1H, -HNMe<sub>2</sub>), 2.68 (s, 6H, -NMe<sub>2</sub>), 2.50 (s, 3H, -Me), 0.43 ppm (s, 9H, TMS); <sup>31</sup>P{<sup>1</sup>H} NMR (142 MHz, CD<sub>3</sub>CN):  $\delta = 252 \text{ ppm}$ .



**Scheme 5.** Formation of **7-d** by treatment of **3** with DCl/D<sub>2</sub>O.

**Synthesis of 5:** **4** (34 mg, 0.1 mmol) was dissolved in refluxing MeCN (0.5 mL) for recrystallization. This resulted in protodesilylation. Yield: 72 % (19 mg, 0.07 mmol).  $^1\text{H}$  NMR (700 MHz,  $\text{CD}_3\text{CN}$ ):  $\delta$  = 7.51–7.41 (m, 5H, *-Ph*), 7.41–7.37 (m, 2H,  $\text{C}_5\text{H}_2\text{P}$ ), 2.75–2.66 (m, 6H, *-NMe\_2*), 2.52 (d,  $^4J_{\text{HP}}$  = 1.5 Hz, 3H, *-Me*), 2.58–2.37 ppm (m, 1H, *-HNMe\_2*);  $^{13}\text{C}\{^1\text{H}\}$  NMR (176 MHz,  $\text{CD}_3\text{CN}$ ):  $\delta$  = 158.9 (d,  $^1J_{\text{CP}}$  = 54 Hz), 146.8 (d,  $^2J_{\text{CP}}$  = 14 Hz), 142.5 (d,  $^2J_{\text{CP}}$  = 12 Hz), 132.0 (d,  $^1J_{\text{CP}}$  = 88 Hz), 130.3 (d,  $^3J_{\text{CP}}$  = 10 Hz), 129.4 (s), 128.3 (s), 125.5 (d,  $^2J_{\text{CP}}$  = 25 Hz), 125.0 (s), 44.8 (s), 24.7 ppm (d,  $^3J_{\text{CP}}$  = 3 Hz);  $^{31}\text{P}\{^1\text{H}\}$  NMR (162 MHz,  $\text{CD}_3\text{CN}$ ):  $\delta$  = 213 ppm; HR-ESI MS (*m/z*): 230.1104 (calcd: 230.1094)  $[\text{M}]^+$ .

**Synthesis of 6:** Compound **3** (36 mg, 0.12 mmol) was dissolved in  $\text{Et}_2\text{O}$  (3 mL) at room temperature, and 0.1 mL HCl in water (0.24 mmol, 2.4 M) was added to the Schlenk flask. The reaction was stirred for overnight before removing all volatiles in vacuo. The residual solid was washed with  $\text{Et}_2\text{O}$ . Yield: 40 % (30 mg, 0.05 mmol).  $^1\text{H}$  NMR (700 MHz,  $\text{D}_2\text{O}$ ):  $\delta$  = 7.68–6.67 (m, 10H, *Ph*), 5.72 (d,  $^3J_{\text{HP}}$  = 24.7 Hz, 2H,  $\text{C}_4\text{HP}$ ), 3.33 (d,  $^3J_{\text{HP}}$  = 11.6 Hz, 4H, *-CH\_2*), 3.01 (s, 9H, *-NMe\_2*), 2.72 (s, 3H, *-NMe\_2*), 2.06 (s, 2H, *-HNMe\_2*), 2.00 (m, 4H,  $\text{CH}_2$ ), 1.76 ppm (s, 6H, *-Me*);  $^{13}\text{C}\{^1\text{H}\}$  NMR (176 MHz,  $\text{D}_2\text{O}$ ):  $\delta$  = 145.0 (d,  $^2J_{\text{CP}}$  = 9 Hz), 134.0 (t,  $^3J_{\text{CP}}$  = 5 Hz), 131.3 (s), 128.3 (s), 127.4 (s), 121.9 (d,  $^2J_{\text{CP}}$  = 17 Hz), 71.3 (d,  $^1J_{\text{CP}}$  = 86 Hz), 40.8 (s), 39.3 (s) 35.1 (d,  $^2J_{\text{CP}}$  = 14 Hz), 35.1 (d,  $^1J_{\text{CP}}$  = 192 Hz), 20.4 ppm (d,  $^3J_{\text{CP}}$  = 12 Hz);  $^{31}\text{P}\{^1\text{H}\}$  NMR (162 MHz,  $\text{D}_2\text{O}$ ):  $\delta$  = 53 ppm;  $^{31}\text{P}$  NMR (162 MHz,  $\text{D}_2\text{O}$ ):  $\delta$  = 53 ppm (t,  $^2J_{\text{HP}}$  = 11 Hz); HR-ESI MS (*m/z*): 531.2596 (calcd: 531.2542)  $[(\text{M} + \text{OH})]^+$ .

**Synthesis of 7:** Compound **3** (72 mg, 0.24 mmol) was dissolved in DCM (3 mL) at room temperature, and HCl in water (0.3 mL, 0.72 mmol, 2.4 M) was added to the Schlenk flask. The reaction was stirred for overnight before removing all volatiles in vacuo. A crystal, suitable for single-crystal X-ray diffraction, was obtained by slowly cooling a hot solution of the crude solid in isopropanol. Yield: 87 % (63 mg, 0.21 mmol).  $^1\text{H}$  NMR (400 MHz,  $\text{D}_2\text{O}$ ):  $\delta$  = 7.55–7.11 (m, 5H, *-Ph*), 5.69 (d,  $^3J_{\text{HP}}$  = 25.3 Hz, 1H, *CH*), 3.29 (d,  $^3J_{\text{HP}}$  = 12.6 Hz, 2H, *-CH\_2*), 2.96 (d,  $^4J_{\text{HP}}$  = 3.4 Hz, 6H, *-NMe\_2*), 2.67 (s, 1H, *-OH*), 2.05–1.96 (m, 1H, *-HNMe\_2*), 1.96 (m, 2H,  $\text{CH}_2$ ), 1.72 ppm (s, 3H, *-CH\_3*);  $^{13}\text{C}\{^1\text{H}\}$  NMR (151 MHz,  $\text{D}_2\text{O}$ ):  $\delta$  = 145.0 (d,  $^2J_{\text{CP}}$  = 9 Hz), 134.0 (d,  $^3J_{\text{CP}}$  = 4 Hz), 131.3 (s), 128.3 (s), 127.4 (s), 121.9 (d,  $^2J_{\text{CP}}$  = 16 Hz), 71.3 (d,  $^1J_{\text{CP}}$  = 86 Hz), 40.8 (s), 39.3 (s), 35.3 (d,  $^1J_{\text{CP}}$  = 95 Hz), 35.2 (s), 20.4 ppm (d,  $^3J_{\text{CP}}$  = 12 Hz);  $^{31}\text{P}\{^1\text{H}\}$  NMR (162 MHz,  $\text{D}_2\text{O}$ ):  $\delta$  = 47 ppm;  $^{31}\text{P}$  NMR (162 MHz,  $\text{D}_2\text{O}$ ):  $\delta$  = 47 ppm (t,  $^2J_{\text{HP}}$  = 25 Hz); HR-ESI MS (*m/z*): 266.1306 (calcd: 266.1304)  $[\text{M}]^+$ .

### Synthesis of 7-TMS-d

**Method 1:** **3** (72 mg, 0.24 mmol) was dissolved in DCM (3 mL) at room temperature, and DCl in  $\text{D}_2\text{O}$  (0.2 mL, 2.4 M) was added to the Schlenk flask. The reaction was stirred for overnight before removing the DCM phase by syringe. The water phase containing the product **7-TMS-d** was washed with 0.2 mL DCM, after which all volatiles were evaporated under vacuum to obtain the pure product. Yield: 62 % (56 mg, 0.15 mmol).

**Method 2:** **3** (72 mg, 0.24 mmol) was dissolved in MeCN or THF (0.5 mL) at room temperature in an NMR tube, and DCl in  $\text{D}_2\text{O}$  (0.2 mL, 2.4 M) was added. This reaction mixture was allowed to stand at room temperature for approximately 5 days. Almost all starting material was converted to the product directly. Yield: 88 % (80 mg, 0.21 mmol). The product was recrystallized from isopropanol without further purification.  $^1\text{H}$  NMR (400 MHz,  $\text{CD}_3\text{CN}$ ):  $\delta$  = 7.43–7.14 (m, 5H, *-Ph*), 5.74 (d,  $^3J_{\text{HP}}$  = 27.1 Hz, 1H, *CH*), 3.00 (s, 6H, *-NMe\_2*), 1.66 (s, 3H, *-Me*), 0.04 ppm (d,  $J$  = 5.6 Hz, 9H, *-TMS*);  $^{13}\text{C}\{^1\text{H}\}$  NMR (151 MHz,  $\text{CD}_3\text{CN}$ ):  $\delta$  = 144.0 (s), 133.8 (s), 132.1 (s), 128.5 (d,  $^2J_{\text{CP}}$  = 14 Hz), 127.9 (s), 122.9 (s), 71.7 (d,  $^1J_{\text{CP}}$  = 90 Hz), 41.7–41.4 (m), 40.3–40.0 (m), 35.7–34.7 (broad peak due to D–C coupling), 20.5 (s),

0.8 (s);  $^{29}\text{Si}\{^1\text{H}\}$ -DEPT NMR (80 MHz,  $\text{CD}_3\text{CN}$ ):  $\delta$  = 8 ppm;  $^{31}\text{P}\{^1\text{H}\}$  NMR (162 MHz,  $\text{CD}_3\text{CN}$ ):  $\delta$  = 55 ppm.

**Synthesis of 7-d:** Protodesilylation of **7-TMS-d** in solution occurs under strong acidic conditions. All volatiles were removed in vacuo after the reaction was completed. The residual solid was dissolved in refluxing isopropanol (0.5 mL) and subsequently recrystallized. Yield: 90 % (58 mg, 0.19 mmol).  $^1\text{H}$  NMR (400 MHz,  $\text{D}_2\text{O}$ ):  $\delta$  = 7.43–7.23 (m, 5H, *-Ph*), 5.67 (dd,  $^3J_{\text{HP}}$  = 24.9, 1.5 Hz, 1H, *CH*), 2.94 (d,  $^2J_{\text{HP}}$  = 3.2 Hz, 6H, *-NMe\_2*), 1.70 (s, 3H, *-Me*) ppm;  $^{13}\text{C}\{^1\text{H}\}$  NMR (151 MHz,  $\text{D}_2\text{O}$ ):  $\delta$  = 145.0 (d,  $^2J_{\text{CP}}$  = 9 Hz), 133.9 (d,  $^3J_{\text{CP}}$  = 4 Hz), 131.3 (s), 128.4 (s), 127.5 (s), 122.0 (d,  $^2J_{\text{CP}}$  = 17 Hz), 71.2 (d,  $^1J_{\text{CP}}$  = 86 Hz), 40.9 (s), 39.3 (s), 36.1–33.7 (m, broad peak due to D–C coupling), 20.4 ppm (d,  $^3J_{\text{CP}}$  = 12 Hz);  $^{31}\text{P}\{^1\text{H}\}$  NMR (162 MHz,  $\text{D}_2\text{O}$ ):  $\delta$  = 48 ppm.

## Supporting Information

All experimental and computational details, including the NMR spectra, can be found in the Supporting Information.

Deposition Numbers 2181743 (**3**), 2181744 (**5**), 2181745 (**6**), 2181746 (**7**) contain the supplementary crystallographic data for this paper. These data are provided free of charge by the joint Cambridge Crystallographic Data Centre and Fachinformationszentrum Karlsruhe Access Structures service.

## Acknowledgements

Funding by the Deutsche Forschungsgemeinschaft (grant PA 1360/16-1) and the China Scholarship Council is gratefully acknowledged. The authors thank the computing facilities of the Freie Universität Berlin (Zentrale Einrichtung für Datenverarbeitung) for providing computational resources. Open Access funding enabled and organized by Projekt DEAL.

## Conflict of Interest

The authors declare no conflict of interest.

## Data Availability Statement

The data that support the findings of this study are available in the supplementary material of this article.

**Keywords:** DFT calculations · phosphinic acid · phospholene · phosphorus heterocycles · X-ray crystallography

- [1] N. T. Coles, A. S. Abels, J. Leitl, R. Wolf, H. Grützmacher, C. Müller, *Coord. Chem. Rev.* **2021**, *433*, 213729–213756.
- [2] a) F. Knoch, F. Kremer, U. Schmidt, U. Zenneck, P. Le Floch, F. Mathey, *Organometallics* **1996**, *15*, 2713–2719; b) P. Le Floch, *Coord. Chem. Rev.* **2006**, *250*, 627–681; c) C. Müller, D. Vogt, *Dalton Trans.* **2007**, 5505–5523; d) C. Müller, D. Vogt in *Catalysis and Material Science Applications, Vol. 36* (Eds.: M. Peruzzini, L. Gonsalvi), Springer, Berlin, **2011**, pp. 151–183; e) M. Rigo, E. R. Habraken, K. Bhattacharyya, M. Weber, A. W. Ehlers, N. Mézailles, J. C. Sloodweg, C. Müller, *Chem. Eur. J.* **2019**, *25*, 8769–8779.
- [3] G. Pfeifer, F. Chahdoura, M. Papke, M. Weber, R. Szűcs, B. Geffroy, D. Tondelier, L. Nyulászi, M. Hissler, C. Müller, *Chem. Eur. J.* **2020**, *26*, 10534–10543.

- [4] a) R. Newland, M. F. Wyatt, R. Wingad, S. M. Mansell, *Dalton Trans.* **2017**, 46, 6172–6176; b) R. J. Newland, M. P. Delve, R. L. Wingad, S. M. Mansell, *New J. Chem.* **2018**, *42*, 19625–19636; c) R. J. Newland, J. M. Lynam, S. M. Mansell, *Chem. Commun.* **2018**, *54*, 5482–5485; d) R. J. Newland, A. Smith, D. M. Smith, N. Fey, M. J. Hanton, S. M. Mansell, *Organometallics* **2018**, *37*, 1062–1073.
- [5] X. Chen, S. Alidori, F. F. Puschmann, G. Santiso-Quinones, Z. Benkő, Z. Li, G. Becker, H. F. Grützmacher, H. Grützmacher, *Angew. Chem. Int. Ed.* **2014**, *53*, 1641–1645; *Angew. Chem.* **2014**, *126*, 1667–1671.
- [6] Y. Hou, Z. Li, Y. Li, P. Liu, C.-Y. Su, F. Puschmann, H. Grützmacher, *Chem. Sci.* **2019**, *10*, 3168–3180.
- [7] S. Giese, K. Klimov, A. Mikeházi, Z. Kelemen, D. S. Frost, S. Steinhauer, P. Müller, L. Nyulászi, C. Müller, *Angew. Chem. Int. Ed.* **2021**, *60*, 3581–3586; *Angew. Chem.* **2021**, *133*, 3625–3630.
- [8] N. Avarvari, P. Le Floch, F. Mathey, *J. Am. Chem. Soc.* **1996**, *118*, 11978–11979.
- [9] F. H. Allen, O. Kennard, D. G. Watson, L. Brammer, A. G. Orpen, R. Taylor, *J. Chem. Soc. Perkin Trans. 2* **1987**, S1–S19.
- [10] F. Wossidlo, D. S. Frost, J. Lin, N. T. Coles, K. Klimov, M. Weber, T. Böttcher, C. Müller, *Chem. Eur. J.* **2021**, *27*, 12788–12795.
- [11] M. H. Habicht, F. Wossidlo, T. Bens, E. A. Pidko, C. Müller, *Chem. Eur. J.* **2018**, *24*, 944–952.
- [12] D. Mootz, W. Poll, H. Wunderlich, H. G. Wussow, *Chem. Ber.* **1981**, *114*, 3499–3504.
- [13] a) F. Leca, C. Lescop, L. Toupet, R. Réau, *Organometallics* **2004**, *23*, 6191–6201; b) R.-M. L. Mercado, C. Zhang, H. Zhang, P. Wisian-Neilson, *Phosphorus Sulfur Silicon Relat. Elem.* **2015**, *190*, 2194–2206.
- [14] a) R. Kohle, W. Kuchen, W. Peters, *Z. Anorg. Allg. Chem.* **1987**, *551*, 179–190; b) J. L. Atwood, S. G. Bott, A. W. Coleman, K. D. Robinson, S. B. Whetstone, C. M. Means, *J. Am. Chem. Soc.* **1987**, *109*, 8100–8101; c) B. H. Ward, G. E. Granroth, K. A. Abboud, M. W. Meisel, D. R. Talham, *Chem. Mater.* **1998**, *10*, 1102–1108; d) K. Nikitin, H. Müller-Bunz, J. Muldoon, D. G. Gilheany, *Chem. Eur. J.* **2017**, *23*, 4794–4802.
- [15] a) J. Grundy, F. Mathey, *Angew. Chem.* **2005**, *117*, 1106–1108; *Angew. Chem. Int. Ed.* **2005**, *44*, 1082–1084; b) H. Wang, C. Li, D. Geng, H. Chen, Z. Duan, F. Mathey, *Chem. Eur. J.* **2010**, *16*, 10659–10661; c) P. Tokarz, P. M. Zagórski, *Chem. Heterocycl. Compd.* **2017**, *53*, 858–860.
- [16] a) S. B. Clendenning, P. B. Hitchcock, J. F. Nixon, L. Nyulászi, *Chem. Commun.* **2000**, 1305–1306; b) S. B. Clendenning, P. B. Hitchcock, M. F. Lappert, P. G. Merle, J. F. Nixon, L. Nyulászi, *Chem. Eur. J.* **2007**, *13*, 7121–7128.
- [17] M. Blug, O. Piechaczyk, M. Fustier, N. Mézailles, P. Le Floch, *J. Org. Chem.* **2008**, *73*, 3258–3261.
- [18] S. Grimme, J. G. Brandenburg, C. Bannwarth, A. Hansen, *J. Chem. Phys.* **2015**, *143*, 054107.
- [19] a) J. P. Perdew, M. Ernzerhof, K. Burke, *J. Chem. Phys.* **1996**, *105*, 9982; b) S. Grimme, J. Antony, S. Ehrlich, H. Krieg, *J. Chem. Phys.* **2010**, *132*, 154104; c) S. Grimme, S. Ehrlich, L. Goerigk, *J. Comput. Chem.* **2011**, *32*, 1456.
- [20] M. Doux, N. Mézailles, L. Ricard, P. Le Floch, *Eur. J. Inorg. Chem.* **2003**, 3878.
- [21] a) B. Schmid, L. M. Venanzi, A. Albinati, F. Mathey, *Inorg. Chem.* **1991**, *30*, 4693; b) I. de Krom, E. A. Pidko, M. Lutz, C. Müller, *Chem. Eur. J.* **2013**, *19*, 7523; c) R. J. Newland, M. P. Delve, R. L. Wingad, S. M. Mansell, *New J. Chem.* **2018**, *42*, 19625.
- [22] a) D. Vincze, P. Ábrányi-Balogh, P. Bagi, G. Keglevich, *Molecules* **2019**, *24*, 3859–3871; b) L. Davis, M. Putri, C. Meyer, C. Durant, *Tetrahedron Lett.* **2014**, *55*, 3100–3103; c) D. Akbayeva, M. Varia, S. S. Costantini, M. Peruzzini, P. Stoppioni, *Dalton Trans.* **2006**, *2*, 389–395.
- [23] J. Baldwin, *J. Chem. Soc. Chem. Commun.* **1976**, *18*, 734–736.
- [24] L. Hong, S. Ahles, M. Strauss, C. Logemann, H. Wegner, *Org. Chem. Front.* **2017**, *4*, 871–875.

---

Manuscript received: November 3, 2022

Accepted manuscript online: November 16, 2022

Version of record online: December 8, 2022